

LA-UR--91-2589

DE91 017820

LA-UR- 91 - 2589

Received by OCTJ

SEP 06 1991

Los Alamos National Laboratory is operated by the University of California for the United States Department of Energy under contract W 7405-ENG-36

TITLE SPONTANEOUS EMISSION FROM FREE ELECTRON LASERS

AUTHOR(S) Mark Jude Schmitt, X-1

SUBMITTED TO SPIE's 1991 International Symposium on Optical Applied Science and Engineering, Short Wavelength Radiation Sources Conference 1552, San Diego, CA, July 21-25, 1991.

DISCLAIMER

This report was prepared as an account of work sponsored by an agency of the United States Government. Neither the United States Government nor any agency thereof, nor any of their employees, makes any warranty, express or implied, or assumes any legal liability or responsibility for the accuracy, completeness, or usefulness of any information, apparatus, product, or process disclosed, or represents that its use would not infringe privately owned rights. Reference herein to any specific commercial product, process, or service by trade name, trademark, manufacturer, or otherwise does not necessarily constitute or imply its endorsement, recommendation, or favoring by the United States Government or any agency thereof. The views and opinions of authors expressed herein do not necessarily state or reflect those of the United States Government or any agency thereof.

By acceptance of this article, the publisher recognizes that the U.S. Government retains a nonexclusive, royalty-free license to publish or reproduce the published form of this contribution, or to allow others to do so, for U.S. Government purposes.

The Los Alamos National Laboratory requests that the publisher identify this article as work performed under the auspices of the U.S. Department of Energy.

DISTRIBUTION OF THIS DOCUMENT IS UNLIMITED  
MASTER

Los Alamos Los Alamos National Laboratory  
Los Alamos, New Mexico 87545

# Spontaneous emission from free electron lasers

Mark J. Schmitt

Los Alamos National Laboratory  
MS F645, Los Alamos, New Mexico 87545 USA

## ABSTRACT

Characteristics of the fundamental and harmonic emission from free-electron lasers (FELs) is examined in the spontaneous emission regime. The radiation at both odd and even harmonic frequencies is treated for electron beams with finite emittance and energy spread. For wigglers with many wiggler periods, calculation of the SE by integrating an ensemble of electrons along their exact trajectories becomes exceedingly cumbersome. Therefore, a different technique is used in which the far-field radiation pattern of a single electron is manipulated in transform space to include the effects of emittance. The effects of energy spread can be included by a weighted sum over the energy distribution. The program execution time for wigglers of arbitrary length is negligible. The transverse radiation patterns including the transverse frequency dependences, are given. How this radiation is modeled in FEL simulation codes is discussed.

## 1. INTRODUCTION

The interest in harmonic radiation from free electron lasers (FELs) has increased in past few years for several important reasons. The level of spontaneous and coherent-spontaneous harmonic power generated during fundamental lasing is of interest from both a mirror damage standpoint and in terms of the use of this radiation for diagnostics and external experimentation. Albeit broadband in frequency, spontaneous emission is the dominant radiation mechanism at the higher harmonics. This radiation diverges faster than the coherent-spontaneous radiation and can suffer significant interception and reflection from the wiggler vacuum tube wall. Its use as an alignment diagnostic can also be important. The prediction of the spontaneous emission power levels for FELs is the subject of this paper.

In Section 2 the mathematical models for the spontaneous emission from a single electron and from an entire electron beam (including emittance effects) are given. Computational examples using these models follows. How spontaneous emission is modeled in the present FEL codes is discussed in Section 3. A brief description of how these models can be used to calculate the spontaneous emission from electromagnetic wigglers is given in Section 4. The conclusions are given in Section 5.

## 2. ANALYTICAL MODEL

Electrons radiate spontaneously in a wiggler. Most of the radiation is contained in a forward directed cone of half angle  $a_w/\gamma$ . The far field radiation intensity for a single electron was analytically derived by Colson<sup>1</sup>. In his derivation he correctly included all terms up to order  $(1/\gamma^2)$ . For a plane-polarized wiggler of length  $L_w = N_w \lambda_w$  and peak magnetic field strength  $B_w$ , driven by an electron beam of energy  $\gamma mc^2$ , the energy radiated by each electron of charge  $q = -e$  per unit solid angle and frequency bandwidth is given by

$$\left. \frac{d^2 I_0}{d\Omega d\omega} \right|_f = \frac{16e^2 N_w^2 \gamma^2}{c} \left( \frac{\sin \nu_f}{\nu_f} \right)^2 \left( \frac{f\xi}{a_w} \right)^2 \left[ \left( \frac{\gamma\theta}{a_w} \right)^2 A_{0,f}^2 + 2 \frac{\gamma\theta}{a_w} \cos \phi A_{0,f} A_{1,f} + A_{1,f}^2 \right] \quad (1)$$

where

$$A_{\alpha,f} = (-1)^{f+\alpha} \sum_{n=-\infty}^{\infty} (-1)^n J_n(f\xi) [J_{f-2n-\alpha}(f\sigma) + J_{f-2n+\alpha}(f\sigma)] \quad (2)$$

$$\nu_f = \pi N_w \left[ f - \frac{\lambda_w}{2\gamma^2 \lambda_s} (1 + a_w^2/2 + \gamma^2 \theta^2) \right] \quad (3)$$

$$f\sigma = \frac{8(f\xi)(\gamma\theta)}{a_w} \cos\phi \quad (4)$$

$$\xi = \frac{a_w^2}{4(1 + a_w^2/2 + \gamma^2\theta^2)} \quad (5)$$

and

$$a_w = \frac{|e|B_w\lambda_w}{2\pi mc^2} \quad (6)$$

is the normalized wiggler magnetic vector potential. The radiation wavelength is  $\lambda_r$ ,  $f$  is the harmonic number and  $J_m(z)$  represents the Bessel function of the first kind of order  $m$ . As depicted in Figure 1, it has been assumed that the wiggler lies along the  $z$ -axis and the observation angles  $\theta$  and  $\phi$  are formed by the intersection of the line of observation, call it  $\hat{n}$ , with the  $z$ -axis and the angle made by the intersection of the projection of  $\hat{n}$  onto the  $xy$ -plane with the  $z$ -axis, respectively. It should be noted that other derivations<sup>2,3</sup> omit an axial phase term, thereby obtaining an erroneous azimuthally symmetric result. The harmonic radiation pattern described in Eq.(1) has multiple lobes where the number of lobes is equal to the harmonic number. A cold electron beam (zero energy spread and emittance) has a radiation pattern that is identical in shape to the single-electron pattern.

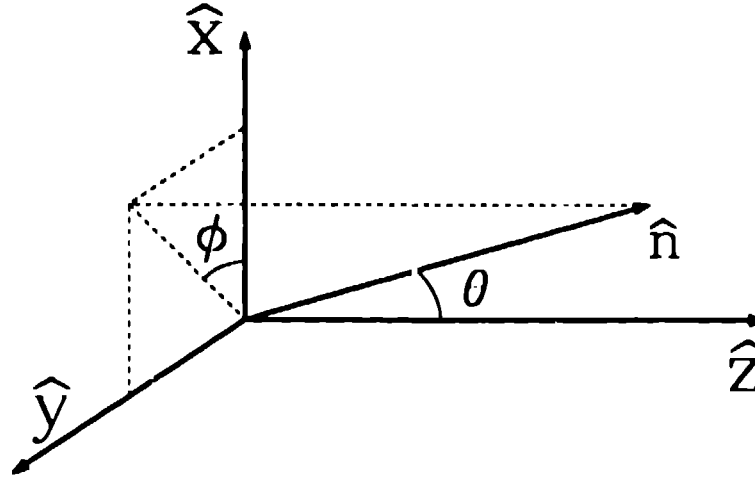


Figure 1. Relation between the cartesian coordinates, the line of observation and the spherical observation angles.

The only frequency dependence in Eq (1) is in the  $\sin^2 \nu_j/\nu_j^2$  term. For  $N_w \gg 1$ , this term is sharply peaked about  $\nu_j = 0$ , where the frequency becomes

$$\omega = \frac{2\gamma^2 f k_w c}{1 + a_w^2/2 + \gamma^2\theta^2} \quad (7)$$

An on-axis observer ( $\theta \Rightarrow 0$ ) sees the frequency

$$\omega_{\text{axis}} = \frac{2\gamma^2 k_w c f}{1 + a_w^2/2} \quad (8)$$

so that, normalizing with respect to this frequency, the relative frequency shift off axis is given by

$$\frac{\omega}{\omega_{\text{axis}}} = \frac{1}{1 + \left(\frac{\gamma^2\theta^2}{1 + a_w^2/2}\right)} \quad (9)$$

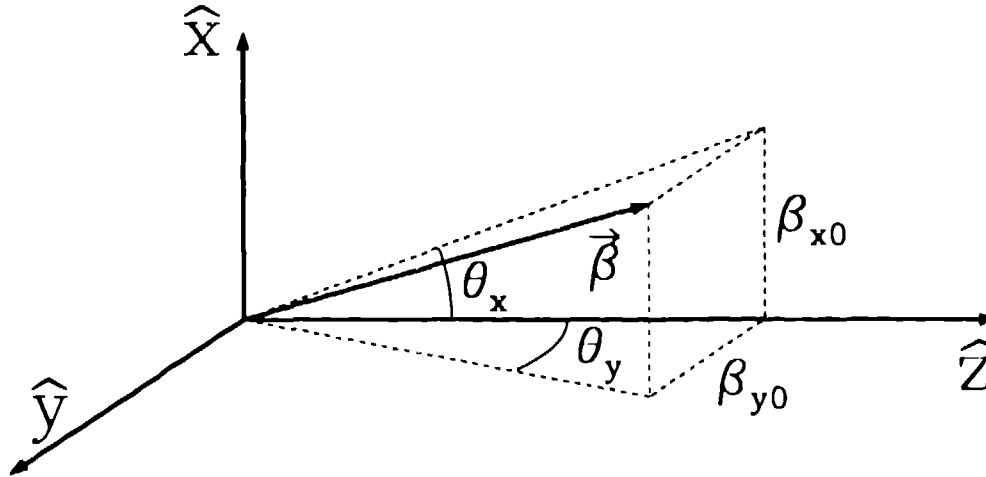


Figure 2. Relation between the electron guiding center velocity,  $\vec{\beta}$ , its transverse drift speeds and the two angles of rotation.

From Eq.(9) one sees that at the edge of the  $\gamma\theta \simeq 1$  cone, the frequency has changed by roughly a factor of two. It should also be noted that since the frequency depends only on  $\theta$  (and not  $\phi$ ), a specific frequency appears spatially as a "frequency ring".

Spontaneous emission from an FEL is composed of the radiation from all the electrons in the electron beam. Since the electron beam has a distribution of electrons in energy, space and transverse velocity, some method must be devised to take these distributions into account in order to obtain the correct spontaneous emission pattern for a non-ideal electron beam. As a first step we can show that the spontaneous emission of an electron with a transverse drift (with respect to the wiggler axis) is identical (to order  $1/\gamma^2$ ) in both intensity and frequency to the spontaneous radiation pattern of the on-axis electron. The only difference is that the drifting electron's radiation pattern is rotated by  $\vec{\beta}_{x0} + \vec{\beta}_{y0}$  away from the wiggler axis where  $\vec{\beta}_{x0}$  and  $\vec{\beta}_{y0}$  correspond to the drift velocities in the  $\hat{x}$  and  $\hat{y}$  directions, respectively. The velocity of an electron in a sinusoidal wiggler field including transverse drift motion is given by

$$\vec{\beta}_e = \begin{pmatrix} \beta_{xe} \\ \beta_{ye} \\ \beta_{ze} \end{pmatrix} = \begin{pmatrix} \frac{a_w}{\gamma} \cos k_w z + \beta_{x0} \\ \beta_{y0} \\ \beta_x - \frac{a_w}{\gamma} \beta_{x0} \cos k_w z - \frac{a_w^2}{4\gamma^2} \cos 2k_w z \end{pmatrix} \quad (10)$$

where

$$\beta_x = 1 - \frac{1 + a_w^2/2}{2\gamma^2} - \beta_{\perp 0}^2/2 \quad (11)$$

and

$$\beta_{\perp 0}^2 = \beta_{x0}^2 + \beta_{y0}^2 \quad (12)$$

as given in Appendix B of reference [4]. We can use a rotation of coordinates to show that to order  $1/\gamma^2$ , the drift terms transform away. This can be done by first performing a rotation in the  $x-z$  plane where the transformed velocities (denoted by  $\prime$ ) are given by

$$\begin{pmatrix} \beta'_{xe} \\ \beta'_{ze} \end{pmatrix} = \begin{pmatrix} \cos \theta_x & -\sin \theta_x \\ \sin \theta_x & \cos \theta_x \end{pmatrix} \begin{pmatrix} \beta_{xe} \\ \beta_{ze} \end{pmatrix} \quad (13)$$

followed by a rotation in the  $y-z$  plane with the transformation

$$\begin{pmatrix} \beta'_{ye} \\ \beta'_{ze} \end{pmatrix} = \begin{pmatrix} \cos \theta_y & -\sin \theta_y \\ \sin \theta_y & \cos \theta_y \end{pmatrix} \begin{pmatrix} \beta_{ye} \\ \beta_{ze} \end{pmatrix} \quad (14)$$

where  $\theta_x$  and  $\theta_y$  are defined in Figure 2.

Combining the two transformations into one<sup>6</sup>, the complete transformation can now be written

$$\begin{aligned} \begin{pmatrix} \beta'_{xe} \\ \beta'_{ye} \\ \beta'_{ze} \end{pmatrix} &= \begin{pmatrix} \cos \theta_x & 0 & -\sin \theta_x \\ 0 & 1 & 0 \\ \sin \theta_x & 0 & \cos \theta_x \end{pmatrix} \begin{pmatrix} 1 & 0 & 0 \\ 0 & \cos \theta_y & -\sin \theta_y \\ 0 & \sin \theta_y & \cos \theta_y \end{pmatrix} \begin{pmatrix} \beta_{xe} \\ \beta_{ye} \\ \beta_{ze} \end{pmatrix} \\ &= \begin{pmatrix} \cos \theta_x & -\sin \theta_x \sin \theta_y & -\sin \theta_x \cos \theta_y \\ 0 & \cos \theta_y & -\sin \theta_y \\ \sin \theta_x & \cos \theta_x \sin \theta_y & \cos \theta_x \cos \theta_y \end{pmatrix} \begin{pmatrix} \beta_{xe} \\ \beta_{ye} \\ \beta_{ze} \end{pmatrix} \end{aligned} \quad (15)$$

Now, since the electron's velocity is mainly in the  $\hat{z}$ -direction, we can approximate

$$\sin \theta_{x,y} \simeq \beta_{x0,y0}/\beta_z \simeq \beta_{x0,y0} \quad (16)$$

and

$$\cos \theta_{x,y} \simeq 1 - \theta_{x,y}^2/2 \simeq 1 - \beta_{x0,y0}^2/2 \quad (17)$$

and denoting  $\beta_x = (a_w/\gamma) \cos k_w z$  and

$$\beta_z = 1 - \frac{1 + a_w^2/2}{2\gamma^2} - \frac{a_w^2}{4\gamma^2} \cos 2k_w z \quad (18)$$

the transformation equation becomes

$$\begin{pmatrix} \beta'_{xe} \\ \beta'_{ye} \\ \beta'_{ze} \end{pmatrix} = \begin{pmatrix} 1 - \beta_{x0}^2/2 & -\beta_{x0}\beta_{y0} & -\beta_{x0} \\ 0 & 1 - \beta_{y0}^2/2 & -\beta_{y0} \\ \beta_{x0} & \beta_{y0} & 1 - \beta_{z0}^2/2 \end{pmatrix} \begin{pmatrix} \beta_x + \beta_{x0} \\ \beta_{y0} \\ \beta_z - \beta_{x0}\beta_x - \beta_{z0}^2/2 \end{pmatrix} = \begin{pmatrix} \beta_x \\ 0 \\ \beta_z \end{pmatrix} \quad (19)$$

where we have kept only terms up to order  $\mathcal{O}(1/\gamma^2)$  and assumed  $\beta_{x0,y0} \propto 1/\gamma$ . As seen from Eq.(19), the drift terms have been transformed away leaving expressions identical to those for an electron on axis. Therefore, the radiation and frequency pattern of a drifting electron is identical to an on-axis electron, with only a shift of the pattern by  $\beta_{z0}$ . (An additional assumption  $\lambda_w \simeq \lambda_w(1 + \beta_{z0}^2/2)$  has also been made.)

With the previous result in mind, we can postulate that the radiation pattern from an ensemble of electrons is given by

$$S(x', y') = \frac{\int dx \int dy e^{-(x^2+y^2)/r^2} \int d\beta_x \int d\beta_y e^{-(\beta_x^2+\beta_y^2)/\beta_z^2} S[x' - (x + \beta_x z), y' - (y + \beta_y z)]}{\int dx \int dy e^{-(x^2+y^2)/r^2} \int d\beta_x \int d\beta_y e^{-(\beta_x^2+\beta_y^2)/\beta_z^2}} \quad (20)$$

where  $S$  is the single-electron radiation pattern and  $z$  is the axial observation point. In Eq.(20), gaussian distributions for the electrons' transverse spatial and velocity dependencies have been assumed. This expression can be manipulated into the form

$$S(x', y') = \mathcal{F}^{-1} \left\{ e^{-2\beta(\beta_z^2 + \beta_{z0}^2)(k_x^2 + k_y^2)} \hat{S}(k_x, k_y) \right\} \quad (21)$$

where  $\mathcal{F}^{-1}\{ \}$  represents the inverse Fourier transform and  $\hat{S}$  is the Fourier transform of  $S$  given by

$$\hat{S}(k_x, k_y) = \int_{-\infty}^{\infty} \int_{-\infty}^{\infty} dx dy S(x, y) e^{-i(k_x x + k_y y)} \quad (22)$$

In the far field we can assume

$$S = \left. \frac{dl}{d\Omega d\omega} \right|_f \quad (23)$$

and  $r = 0$  so that the radiation pattern for the electron beam becomes

$$S(x', y') = \mathcal{F}^{-1} \left\{ e^{-2\beta\beta_z^2(k_x^2 + k_y^2)} \left. \frac{dl}{d\Omega d\omega} \right|_f \right\} \quad (24)$$

where again, the tilde represents the transformed quantity. Using Eqs.(1)-(6) and (24) the spontaneous emission for a single electron or an entire electron beam with a given energy spread and emittance can be obtained.

The previously described spontaneous emission model has been incorporated into the code SPEMIT. A finite summation is performed providing an excellent approximation for Eq(2). After Eq(1) has been calculated on an  $x$ - $y$  grid, an FFT routine is used to obtain its Fourier transform. Multiplication by the angular divergence factor is then performed, after which the FFT routine is used to perform the inverse transform yielding the radiation pattern for the electron ensemble. An example of the code output is given in Figure 3. Here the far-field single-electron radiation pattern at the sixth harmonic is depicted for the 5.0 meter wiggler on the Argonne Advanced Photon Source (APS). Other parameters used for the simulation were:  $\lambda_w = 3.3\text{cm}$ ,  $\gamma = 13700$ ,  $B_w = 3788.0$  Gauss, and  $I = 0.1$  Amps. The frequency dependence, as given in Eq.(7), is shown as color variation over the plot. Note that the number of maxima is equal to the harmonic number.

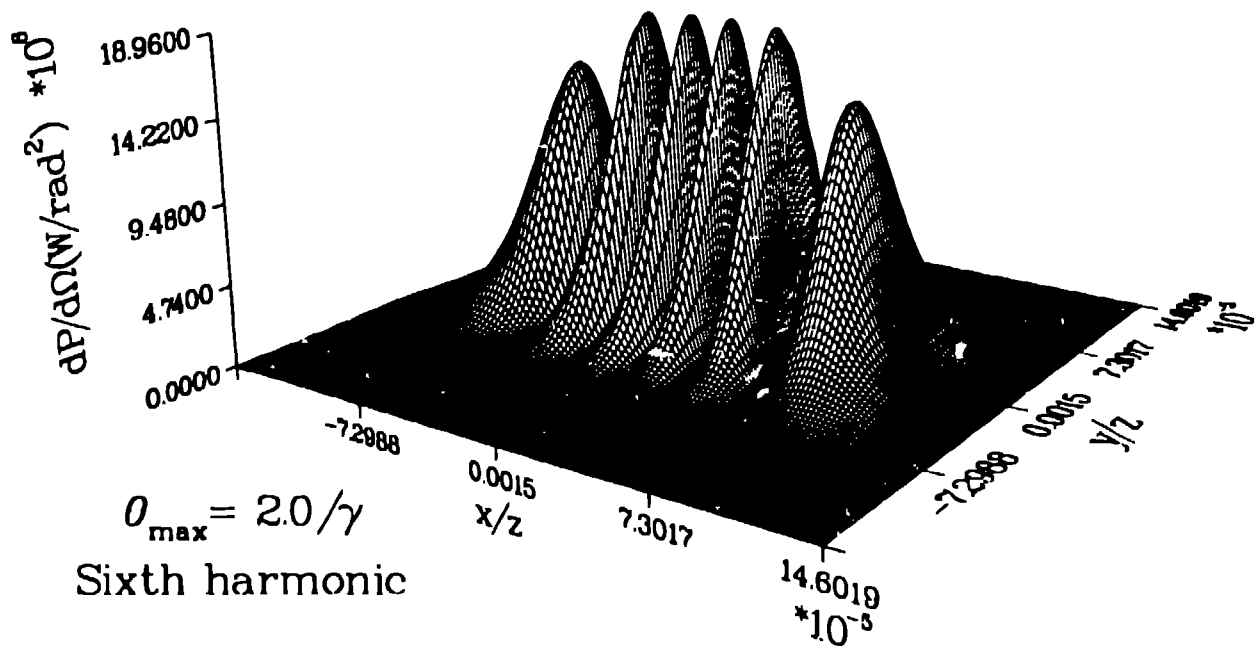
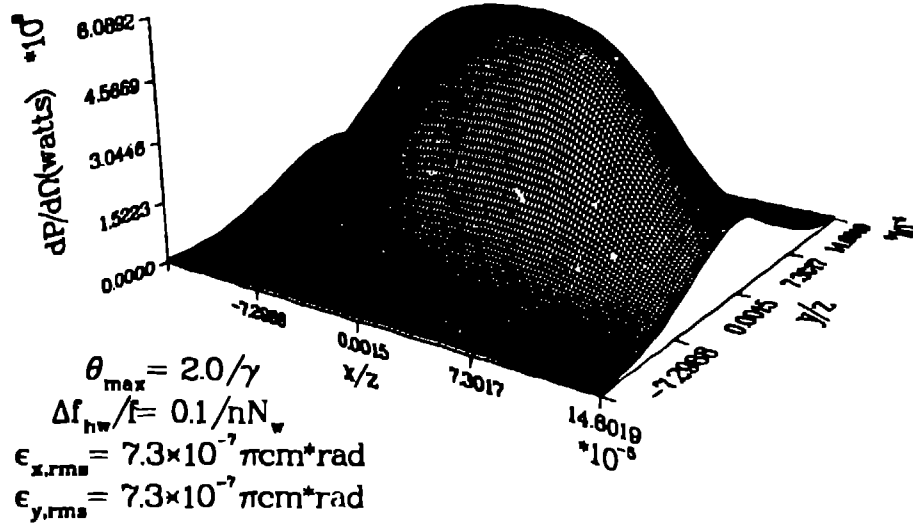


Figure 3. Plot of the single-electron spontaneous emission pattern at the sixth harmonic for the Argonne APS wiggler. Frequency changes are depicted in color.

The spontaneous emission pattern for the entire electron beam can also be calculated. When emittance effects are included ( $\epsilon = 4.5 \times 10^{-6}$  cm-rad gaussian  $1/e$ ), the radiation pattern evolves from that given in Figure 3 for the single electron to that given in Figure 4 for the electron ensemble. Note that the fine structure has been washed out by the electron's transverse velocity distribution. The spontaneous emission power for an FEL should always be calculated since it may exceed the coherent-spontaneous power in devices with poor emittance.

### 3. SIMULATION OF NOISE IN FELP AND FELEX

In a free electron laser (FEL) the number of electrons per wavelength is fixed by the beam current. Upon entering the wiggler, each electron can be assigned a phase with respect to the co-propagating ponderomotive wave



**Figure 4.** Spatial plot of the sixth harmonic spontaneous emission intensity for the Argonne APS wiggler. The distribution of transverse velocities due to emittance has smeared the single-electron pattern.

traveling at slightly less than the electron's axial speed. Variations in the electron current can therefore be mapped into variations in the axial electron density in phase space. This variation gives rise to shot noise. This noise is different from quantum noise which arises due to the random temporal emission of photons by each electron inside the wiggler. This analysis does not include any quantum noise effects which others have shown<sup>6</sup> to be negligible in our regime of interest.

For our purposes we can assume the ponderomotive wavelength is equal to the optical field wavelength (high- $\gamma$  approximation). The contribution from each electron to the optical wave can be modeled by a complex phasor given by<sup>7</sup>

$$t_i = \alpha_i e^{i\phi_i} \quad (25)$$

where  $\alpha_i$  is the amplitude of the phasor representing the  $i^{\text{th}}$  electron ( $\alpha_i \propto q_i/\gamma_i$ ) and  $\phi_i$  is its phase. Denoting the number of electrons per optical wavelength as  $N_e$ , the resultant phasor is given by

$$t = \sum_{i=1}^{N_e} \alpha_i e^{i\phi_i} \quad (26)$$

where the phase of  $t$  will determine how the macroscopic optical electric field is driven<sup>4</sup>. In the case of a FEL,  $\alpha_i$  is inversely proportional to the individual electron energy,  $\gamma_i$ . We assume here that the electron beam energy spread is small,  $\Delta\gamma/\gamma \ll 1$  such that all electrons have equal amplitude.

The real and imaginary parts of  $t$  are just

$$\begin{bmatrix} r \\ i \end{bmatrix} = \sum_{i=1}^{N_e} \alpha_i \begin{bmatrix} \cos \phi_i \\ \sin \phi_i \end{bmatrix} \quad (27)$$

We assume here that  $\phi_i$  is randomly distributed from  $-\pi$  to  $\pi$  such that

$$\overline{\cos \phi_i} = \overline{\sin \phi_i} = 0 \quad (28)$$

where the bar denotes the average value of  $\cos \phi_i$ . It follows trivially that

$$\overline{\begin{bmatrix} \bar{r} \\ \bar{i} \end{bmatrix}} = \sum_{i=1}^{N_e} \overline{\alpha_i} \begin{bmatrix} \overline{\cos \phi_i} \\ \overline{\sin \phi_i} \end{bmatrix} = 0 \quad (29)$$

where the averaging process should not be confused with the sum over  $i$  and we have used the fact that  $\bar{\alpha}_i = \bar{\alpha}_n = \bar{\alpha}$ . Evaluating the second moments we have

$$\overline{r^2} = \sum_{i=1}^{N_e} \sum_{j=1}^{N_e} \overline{\alpha_i \alpha_j \cos \phi_i \cos \phi_j} \quad (30)$$

$$\overline{i^2} = \sum_{i=1}^{N_e} \sum_{j=1}^{N_e} \overline{\alpha_i \alpha_j \sin \phi_i \sin \phi_j} \quad (31)$$

and since the amplitudes and phases are all independent of one another we can write

$$\overline{\cos \phi_i \cos \phi_j} = \begin{cases} \overline{\cos \phi_i} \overline{\cos \phi_j} = 0 & \text{for } i \neq j \\ \overline{\cos^2 \phi_i} = 1/2 & \text{for } i = j \end{cases}$$

and similarly for the sin terms, such that

$$\begin{aligned} \overline{r^2} = \overline{i^2} &= \sum_{i=1}^{N_e} \frac{\overline{\alpha_i \alpha_i}}{2} \\ &= \sum_{i=1}^{N_e} \frac{\overline{\alpha^2}}{2}. \end{aligned} \quad (32)$$

For our case, all vectors (electrons) have essentially equal amplitude ( $\gamma_i \simeq \gamma_0$ ,  $q_i = -e$ ) so that

$$\overline{r^2} = \overline{i^2} = \frac{N_e \overline{\alpha^2}}{2}. \quad (33)$$

For any random variable the variance is given by

$$\sigma^2 = \overline{u^2} - \bar{u}^2 \quad (34)$$

so that using Eqs.(29), (33) and (34) the variance for the real part (or imaginary part) of  $t$  is given by

$$\sigma_e^2 = \frac{N_e \overline{\alpha^2}}{2} \quad (35)$$

where the  $e$  subscript signifies that this is the experimental (or physical) variance.

In the simulation codes (FELP and FELEX<sup>8</sup>), "sets" of electrons are initialized uniformly in phase between 0 and  $2\pi$  such that, for each set containing  $N_p$  electrons

$$t_k = \sum_{k=1}^{N_p} \alpha e^{i\psi_k} = 0 \quad (36)$$

so that each set is "quiet", i.e., it produces no noise. Here  $\alpha$  is a constant independent of  $k$  since the electrons in each set have identical energy. These vectors are commonly referred to as *lattice vectors* due to their periodic spacing in phase. To add noise to the problem we can randomly displace the electrons about their initial lattice positions.

Mathematically, this is accomplished by rotating each lattice vector by a small amount,  $\delta\psi_k$ , so that, for each set of electrons

$$t_s = \sum_{k=1}^{N_p} \alpha e^{i(\psi_k + \delta\psi_k)} \neq 0 \quad (37)$$

which can be approximated for small  $\delta\psi_k$  as

$$t_s = \sum_{k=1}^{N_p} \alpha e^{i\psi_k} (1 + i\delta\psi_k) \quad (38)$$

where  $\delta\psi_k$  is the initial phase displacement of the  $k$ th electron. Assuming  $N_s$  sets of electrons are modeled, the resultant phasor (representing all the simulation electrons) is given by

$$t = \sum_{l=1}^{N_s} \sum_{k=1}^{N_p} \alpha_l [e^{i\psi_k} (1 + i\delta\psi_k)]_l \quad (39)$$

where the orientation between  $N_s$  sets in phase is random. Using Eq.(36) and defining  $\bar{\psi}_k = \psi_k + \pi/2$ , this expression reduces to

$$t = \sum_{l=1}^{N_s} \sum_{k=1}^{N_p} \alpha_l [\delta\psi_k e^{i\bar{\psi}_k}]_l \quad (40)$$

and letting the total number of simulation electrons,  $N_t = N_s N_p$ , gives

$$t = \sum_{k=1}^{N_t} \alpha_s \delta\psi_k e^{i\bar{\psi}_k} \quad (41)$$

where we assumed  $\alpha_l = \alpha_s$  is a constant. This equation has the same form as Eq.(26) for the experimental case. Therefore, we can use Eqs.(32) and (34) to obtain

$$\begin{aligned} \sigma_s^2 &= N_t \overline{\alpha_s^2} \frac{\overline{\delta\psi^2}}{2} \\ &= N_t \alpha^2 \left(\frac{N_e}{N_t}\right)^2 \frac{\overline{\delta\psi^2}}{2} \end{aligned} \quad (42)$$

where  $\alpha_s$ , the amplitude of the simulation electron phasor, has been replaced by the number of experimental electrons it represents

$$\alpha_s = \alpha \left(\frac{N_e}{N_t}\right) \propto \frac{-e}{70} \left(\frac{N_e}{N_t}\right) \quad (43)$$

in order to obtain the correct macroscopic current.

Since both the real FEL and the system model contain many electrons, both of their probability density functions must obey Gaussian statistics as a consequence of the central limit theorem. Therefore, we want to adjust  $\overline{\delta\psi^2}$  such that the same amount of power is radiated for both cases.

To obtain identical statistics for both the experiment and simulation, we equate the variances for the two cases and solve for  $\overline{\delta\psi^2}$ , the initial rms phase displacement. Using Eqs.(35) and (42) gives

$$\frac{N_e}{2} = N_t \left(\frac{N_e}{N_t}\right)^2 \frac{\overline{\delta\psi^2}}{2} \quad (44)$$

or

$$\delta\psi_{rms} = \sqrt{\overline{\delta\psi^2}} = \left(\frac{N_t}{N_e}\right)^{1/2} \quad (45)$$

For the harmonics where  $N_e \rightarrow N_e/f$ ,  $N_t \rightarrow N_t/f$ , and  $\psi_k \rightarrow f\psi_k$  the rms harmonic phase noise is given by

$$f\delta\psi_{rms} = \left(\frac{N_t}{fN_e}\right)^{1/2}. \quad (46)$$

Thus, the standard deviation of the simulation electrons from their uniform positions should be much less than the  $-\pi$  to  $\pi$  variation that exists when all the electrons are simulated. This insures that the simulation electric-field noise in the forward direction will be equivalent to spontaneous emission in the experiment. Note that when simulating the harmonic radiation,  $N_p$  must be adjusted so that Eq.(36) holds for the harmonic of interest. This can easily be accomplished by setting  $N_p$  equal to twice the harmonic number.

For multi-dimensional simulations, radial noise arises in the transverse field profile due to the fluctuations in the axial phase average ( $t$ ) for different transverse locations. The wavelength of the light being simulated determines the minimum structure size of these fluctuations. Thus, the transverse grid spacing should be roughly equal to the optical wavelength for the proper radial averaging to take place. Coarser grid spacing would presumably over estimate this averaging thereby requiring a longer time for the laser to start up.

A question often arises regarding the noise observed off-axis from a set of electrons initialized uniformly on axis (quiet). This picture is inconsistent with the way the electric field is calculated, i.e.

$$E \propto \left\langle \frac{e^{i\psi}}{\gamma} \right\rangle_{e^-} \quad (47)$$

so that the electric field source at any transverse location depends only on the axial location of the electrons at that transverse location. Additional off-axis field contributions from diffraction are then calculated by the field propagator.

The normalized spectral intensity calculated using Eq.(45) in the one dimensional FEL code FELP is given in Figure 5. This data was generated by averaging the spectral intensities from many passes thereby allowing the simulation to be conducted with relatively few simulation electrons per pass. The results reproduce the  $\sin^2 x/x^2$  behavior exhibited in Eq.(1). Parameters for the simulation were;  $\lambda_w = 1$  cm,  $B_w = 12000$  Gauss,  $\gamma = 370$ ,  $I_{peak} = 125$  Amps. The electron beam was assumed to be cold so that the spectral fringes would be well defined. Using this model, calculation of the spectral lineshapes for tapered wigglers and/or electron beams with emittance and energy spread is possible. Further three dimensional calculations (FELEX) are planned to compare the angular power spectrum with the analytical model.

#### 4. ELECTROMAGNETIC WIGGLERS

The models for spontaneous emission described in Sections 2 and 3 assumed wigglers constructed of magnetic materials. However, these models can also valid for FEL interactions where the wiggler consists of an electromagnetic wave, provided some simple modifications are made to the model. An electromagnetic wave colliding with an electron beam produces a sinusoidal oscillation of the electrons. In the high gamma limit, this motion is identical to that induced by a magnetic wiggler with

$$\lambda_w = \lambda_{em}/2 \quad (48)$$

where  $\lambda_w$  is the magnetic wiggler period and  $\lambda_{em}$  is the wavelength of the optical wiggler field. The analogous effective wiggler vector potential is given by

$$a_w = 8.6 \times 10^{-6} \sqrt{\frac{P_{wig}(W)\lambda_{em}}{z_r}} \quad (49)$$

where  $P_{wig}$  is the optical wiggler power and  $z_r$  is the Rayleigh range of the optical wiggler field in the interaction region. The equivalent wiggler magnetic field,  $B_w$ , is given by

$$B_w = \frac{a_w}{.9337\lambda_w}. \quad (50)$$

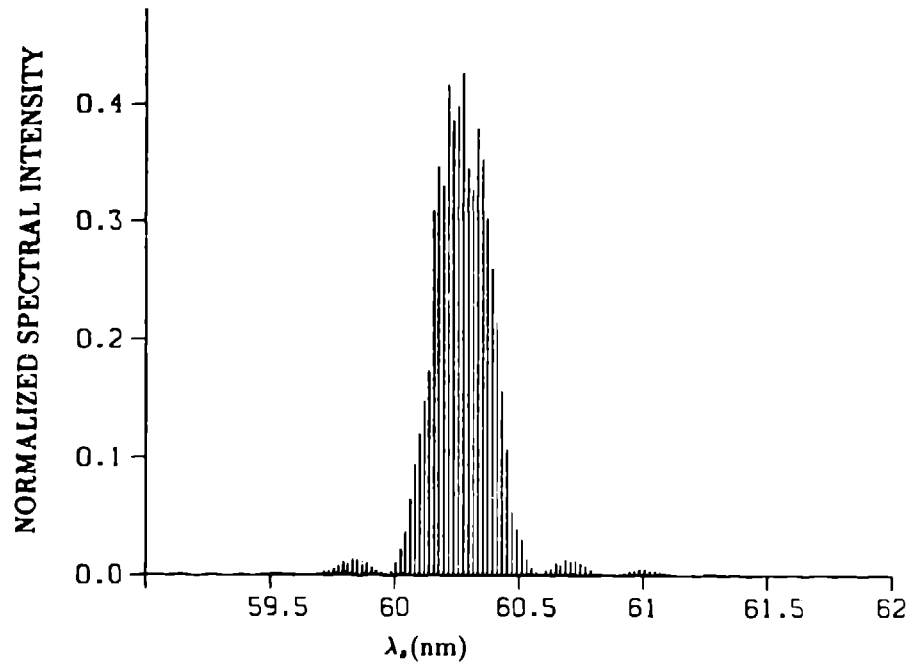


**Figure 5.** Spectral intensity generated with electron phase jitter in the one dimensional FEL code FELP. The intensity envelope is in excellent agreement with Eq.(1) for  $\theta = 0$ .

Several modifications to the simulation codes are required to properly model electromagnetic wigglers. The cosh transverse dependence of a magnetic wiggler must be replaced with the gaussian dependence of an optical wiggler. The spotsize of the optical wiggler must be judiciously chosen (e.g. some multiple of the electron beam radius). A thorough model would also include the gaussian amplitude and phase dependence of the optical wiggler field. The focusing effects of the magnetic wiggler must also be removed from the electron equations of motion.

## 5. CONCLUSIONS

The ability to model spontaneous emission from FELs has been demonstrated. The models are three-dimensional in nature and include the effects of energy spread and emittance. The frequency lineshape of the spontaneous emission generated by electron beams with arbitrary emittance and energy spread in wigglers with tapered or untapered profiles can be obtained by using the electron noise model in the FEL simulation codes. With a few modifications these codes can also be used to model the spontaneous emission from electromagnetic wigglers. Addition work to model spontaneous emission with the simulation code FELEX is planned.

## 6. ACKNOWLEDGMENTS

The author would like to thank John Goldstein and Brian McVey for useful discussions on the topics covered in this paper.

## 7. REFERENCES

1. W. B. Colson, G. Dattoli and F. Ciocci, "Angular-gain Spectrum of Free-electron Lasers", Phys. Rev. A, **31**, pp. 828-842, (1985).
2. B. M. Kincaid, "Random Errors in Undulators and Their Effects on the Radiation Spectrum", J. Opt. Soc.

- Am. B 2 pp. 1294-1306, 1935.
3. S. Krinsky, "Undulators as Sources of Synchrotron Radiation", IEEE Trans. on Nuclear Science, NS-30, pp. 3078-3082, 1983.
  4. M. J. Schmitt and C. J. Elliott, "Generalized Derivation of Free-electron-laser Harmonic Radiation from Plane-polarized Wigglers", Phys. Rev. A41, pp. 3853-3866, 1990.
  5. H. Goldstein, Classical Mechanics, Section 4.4, Addison-Wesley Publishing Company, Reading, Massachusetts, 1950.
  6. S. Benson and J. M. J. Madey, "Shot and Quantum Noise in Free Electron Lasers", Nucl. Instrum. Methods Phys. Res. A237, J. M. J. Madey and A. Renieri editors, pp. 55-60, North-Holland, Amsterdam, 1985.
  7. This derivation closely follows that given in Section 2.9 of J. Goodman, Statistical Optics, Wiley, New York, New York, 1985.
  8. B. D. McVey, J. C. Goldstein, R. L. Tokar, C. J. Elliott, S. J. Gitomer, M. J. Schmitt, and L. E. Thode, "Numerical Simulations of Free-Electron Laser Oscillators", Nucl. Instrum. Methods Phys. Res., A285, A. Gover and V. Granatstein editors, pp. 186-191, North-Holland, Amsterdam, 1989.